Department of Biochemistry, University of Sydney, for the ultracentrifuge runs.

Registry No. DPC, 29557-51-5.

REFERENCES

Bloom, M., & Smith, I. C. P. (1985) in *Progress in Protein–Lipid Interactions* (Watts, A., & De Pont, R., Eds.) Chapter 2, Elsevier, Amsterdam.

Boggs, J. M., & Moscarello, M. A. (1978a) *J. Membr. Biol. 39*, 75–96.

Boggs, J. M., & Moscarello, M. A. (1978b) *Biochim. Biophys. Acta 515*, 1–21.

Boggs, J. M., Moscarello, M. A., & Paphadjopoulos, D. (1982) in *Lipid–Protein Interactions* (Jost, P. C., & Griffith, O. H., Eds.) Vol. II, Chapter 1, Wiley-Interscience, New York.

Bösch, C., Brown, L. R., & Wüthrich, K. (1980) *Biochim. Biophys. Acta 603*, 298–312.

Brown, L. R. (1979) *Biochim. Biophys. Acta 557*, 135–148.

Brown, L. R., Bösch, C., & Wüthrich, K. (1981) *Biochim. Biophys. Acta 642*, 296–312.

Cannon, B., Polnaszek, C. F., Butler, K. W., Eriksson, L. E. G., & Smith, I. C. P. (1975) *Arch. Biochem. Biophys. 267*, 505–518.

Carr, H. Y., & Purcell, E. M. (1954) *Phys. Rev. 94*, 630.

Epand, R. M., Moscarello, M. A., Ziereuberg, B., & Vail, W. J. (1974) *Biochemistry 13*, 1264–1267.

Eylar, E. H., Salk, J., Beveridge, G. L., & Brown, L. V. (1969) *Arch. Biochem. Biophys. 132*, 34–48.

Griffith, O. H., & Jost, P. C. (1976) in *Spin Labelling—Theory and Applications* (Berliner, L. J., Ed.) Chapter 12, Academic, New York.

Koppel, D. E. (1972) *J. Chem. Phys. 57*, 4814–4820.

Lauterwein, J., Bösch, C., Brown, L. R., & Wüthrich, K. (1979) *Biochim. Biophys. Acta 556*, 244–264.

Mendz, G. L., Moore, W. J., Brown, L. R., & Martenson, R. E. (1984) *Biochemistry 23*, 6041–6046.

Reynolds, J. A., & Tanford, C. (1976) *Proc. Natl. Acad. Sci. U.S.A. 73*, 4467–4470.

Sakurai, I. (1985) *Biochim. Biophys. Acta 815*, 149–152.

Sakurai, I., & Kawamura, Y. (1984) *Biochim. Biophys. Acta 777*, 347–351.

Sixl, F., Brophy, P. J., & Watts, A. (1984) *Biochemistry 23*, 2032–2039.

Smith, R. (1985) *Febs Lett. 183*, 331–334.

Stone, R. J., Buckman, T., Nordio, P. L., & McConnell, H. M. (1965) *Proc. Natl. Acad. Sci. U.S.A. 54*, 1010–1017.

Fluorescent Probes of Electrostatic Potential 1 nm from the Membrane Surface†

Anthony P. Winiski,‡ Moises Eisenberg,§ Marek Langner,∥ and Stuart McLaughlin*,∥

Departments of Biochemistry, Pharmacological Sciences, and Physiology and Biophysics, State University of New York, Stony Brook, New York 11794

Received May 20, 1987; Revised Manuscript Received August 18, 1987

ABSTRACT: We measured the electrostatic potential 1 nm from the surface of charged phospholipid bilayer membranes to test the predictions of the Gouy–Chapman theory. Fluorescent probes (anthraniloyl, 5-(dimethylamino)naphthalene-1-sulfonyl, Lucifer yellow) were attached covalently to the sialic acid residue of the ganglioside galactosyl-*N*-acetylgalactosaminyl(*N*-acetylneuraminyl)galactosylglucosylceramide (G_{M1}). These fluorescent gangliosides were incorporated into neutral [phosphatidylcholine (PC)] or charged [phosphatidylserine (PS)] phospholipid bilayers, and the fluorescence was quenched with the cations thallium and 4-amino-2,2,6,6-tetramethylpiperidine-1-oxyl (tempamine). We calculated the electrostatic potential at the chromophore from the quenching ratio using the Boltzmann relation: the average potential was −30 mV for PS bilayers in 0.1 M $NaNO_3$. We assume the chromophore is 1 nm from the surface because X-ray diffraction measurements demonstrate that the sialic acid residue of G_{M1} is 1 nm from the surface of a PC/G_{M1} bilayer [McDaniel, R. V., & McIntosh, T. J. (1986) *Biophys. J. 49*, 94–96]. We also used thallium and tempamine to quench the fluorescence of chromophores located at the surface of the PS membranes; in 0.1 M $NaNO_3$ the average surface potential was −80 mV, which agrees with other measurements. The Gouy–Chapman theory predicts that the potential 1 nm from a membrane with a surface potential of −80 mV is −24 mV; this prediction agrees qualitatively with the experimental results obtained with fluorescent gangliosides.

The Gouy–Chapman theory describes how the electrostatic potential in the aqueous phase at the surface of a bilayer membrane, ψ_0, should depend on the surface charge density, σ, and monovalent salt concentration, C. When ψ_0 is small

$$\psi_0 = \sigma/(\epsilon_r \epsilon_0 \kappa) \quad (1)$$

where ϵ_r is the dielectric constant of the aqueous solution, ϵ_0 is the permittivity of free space, and $1/\kappa$ is the Debye length, which is proportional to $C^{-1/2}$ and equal to 1 nm for $C = 0.1$ M. Several different experimental techniques demonstrate the Gouy–Chapman theory describes adequately the dependence of ψ_0 on σ and C (Hartley & Roe, 1940; Davies, 1951; McLaughlin, 1977; Eisenberg et al., 1979; Cafiso & Hubbell, 1981; Hartsel & Cafiso, 1986; Winiski et al., 1986).

† This work was supported by National Science Foundation Grant BNS 85-01456, National Institutes of Health Grant GM 24971, and Anna Fuller Foundation Fellowship 667.

‡ Department of Biochemistry.

§ Department of Pharmacological Sciences.

∥ Department of Physiology and Biophysics.

0006-2960/88/0427-0386$01.50/0

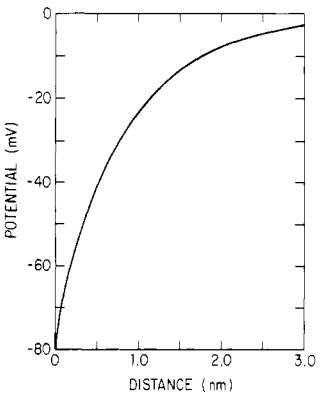

FIGURE 1: Electrostatic potential, $\psi(x)$, calculated from nonlinear Gouy–Chapman theory (eq 2). $\psi(x)$ is plotted as a function of distance from the membrane. The aqueous solution contains 0.1 M monovalent salt; $1/\kappa$ = 0.96 nm at 25 °C.

The Gouy–Chapman theory also describes how the potential, $\psi(x)$, should vary with distance from the surface, x, in a monovalent electrolyte solution (see Figure 1)

$$\psi(x) = \frac{2RT}{\mathcal{F}} \ln \frac{(1 + \alpha \exp(-\kappa x))}{(1 - \alpha \exp(-\kappa x))} \quad (2)$$

where

$$\alpha = \frac{\exp(\mathcal{F}\psi_0/2RT) - 1}{\exp(\mathcal{F}\psi_0/2RT) + 1} \quad (3)$$

T is the absolute temperature, R is the gas constant, and $\mathcal{F}$ is the Faraday constant. For small potentials, $\psi_0 < RT/\mathcal{F} \sim$ 25 mV, eq 2 may be approximated by

$$\psi(x) = \psi_0 \exp(-\kappa x) \quad (4)$$

Two techniques have been used to provide definitive tests of eq 2. Measurements of the force and distance between bilayer surfaces (Marra & Israelachvili, 1985; Marra, 1986; Pashley et al., 1986) and X-ray diffraction estimates of the distance between bilayers when the force is known (Loosley-Millman et al., 1982; Evans & Parsegian, 1986) both demonstrate that for separation distances >2 nm eq 2 describes the potential very accurately. Unfortunately, these techniques cannot be used to measure the dependence of potential on distance from a phospholipid bilayer for x <2 nm: the large forces tend to warp the mica sheets used as substrates for the bilayer in the Israelachvili apparatus (Marra, 1986) and, more importantly, a force of unknown origin, the "hydration force", overwhelms the electrostatic repulsion for x <2 nm [e.g., Loosley-Millman et al. (1982) and Israelachvili (1985)]. Thus, there is a gap in our knowledge of how the potential adjacent to a phospholipid membrane varies with distance.

Hentschel et al. (1985) approached the problem by making neutron diffraction measurements of the concentration profile of deuteriated tetramethylammonium ions between negatively charged phosphatidylglycerol (PG)[1] lipid bilayers. Their approach is direct, and the experimentally measured profiles agree with the values predicted by the Gouy–Chapman theory, but the resolution is very poor. We think other new approaches must be developed to provide an adequate experimental description of the potential profile and concentration of counterions for x <2 nm.

Altstiel and Landsberger (1987) have used an electron spin resonance technique to estimate the potential as a function of distance from a charged phospholipid bilayer. pH indicator dyes confined to an interface have long been used to measure the surface pH and deduce the surface potential (Hartley & Roe, 1940; Fromherz, 1973; Fromherz & Masters, 1974; Vaz et al., 1978). Fromherz (1987) reviewed the use of membrane-bound fluorescent pH indicators to estimate surface potentials of lipid bilayers. We considered using fluorescent pH indicators to map out the potential profile adjacent to a bilayer. However, we want ultimately to investigate the potential profile adjacent to a biological membrane, and one disadvantage of using the pH indicator technique is the many titratable groups on biological membranes.

We have explored a similar technique, fluorescence quenching. We placed a fluorescent probe at a known location near the membrane–solution interface and quenched its fluorescence with monovalent cations. The quenching is proportional to the concentration of charged quencher, Q, adjacent to the fluorophore, $[Q]_f$. The Boltzmann relation predicts

$$[Q]_f = [Q]_\infty \exp(-\mathcal{F}\psi_f/RT) \quad (5)$$

where $[Q]_\infty$ is the concentration of the quencher in the bulk aqueous phase and ψ_f is the electrostatic potential sensed by the quenchers adjacent to the fluorophore.

We attached fluorescent probes to the sialic acid residue of the ganglioside G_{M1}, which is about 1 nm from the surface of a PC/G_{M1} bilayer on the basis of on X-ray diffraction experiments (McDaniel & McIntosh, 1986), monolayer measurements (Maggio, 1985; Maggio et al., 1981), and theoretical calculations (Wynn & Robson, 1986). We assume the probes are also 1 nm from the surface. We incorporated the fluorescent gangliosides into neutral (PC) and charged (PS) phospholipid bilayers and quenched the fluorescence with the cations thallium and tempamine. We also used this technique to measure the surface potential of charged phospholipid bilayers by employing fluorophores that are known to be located at the membrane surface.

An experimental description of the potential profile in a solution containing electrolytes should be of interest to biophysicists studying channels in membranes [e.g., Coronado (1986)], to biochemists examining the role of electrostatics in enzyme kinetics [e.g., Klapper et al. (1986)], and to theoreticians developing sophisticated new models of the electrostatic diffuse double layer [e.g., Kjellander and Marcelja (1986)].

Materials and Methods

Egg phosphatidylcholine (PC), bovine brain phosphatidylserine (PS), egg phosphatidylglycerol (PG), egg *N*-(7-nitro-2,1,3-benzoxadiazol-4-yl)phosphatidylethanolamine (NBD-PE), and egg *N*-(1-pyrenesulfonyl)phosphatidylethanolamine (pyrene-PE) were obtained from Avanti Biochemicals (Birmingham, AL). 4-Morpholinepropanesulfonic acid (MOPS) was obtained from P-L Biochemicals (Milwaukee, WI). Gramicidin D and sodium periodate were obtained from Sigma (St. Louis, MO); sodium cyanoborohydride and potassium borohydride from Aldrich (Milwaukee, WI); and 2-(hexadecylamino)naphthalene-6-sulfonate (HNS), [5-(dimethylamino)naphthalene-1-sulfonyl]hydrazine (dansylhydrazine), anthraniloylhydrazine, Lucifer yellow carbohydrazide, 4-amino-2,2,6,6-tetramethylpiperidine-1-oxyl

[1] Abbreviations: ANT, anthraniloyl; CH, carbohydrazide; dansyl, 5-(dimethylamino)naphthalene-1-sulfonyl; G_{M1}, galactosyl-*N*-acetylgalactosaminyl(*N*-acetylneuraminyl)galactosylglucosylceramide; MOPS, 4-morpholinepropanesulfonate; HNS, 2-(hexadecylamino)naphthalene-6-sulfonate; LY, Lucifer yellow; NBD-PE, egg *N*-(7-nitro-2,1,3-benzoxadiazol-4-yl)phosphatidylethanolamine; PC, phosphatidylcholine; PG, phosphatidylglycerol; PS, phosphatidylserine; pyrene-PE, egg *N*-(1-pyrenesulfonyl)phosphatidylethanolamine; tempamine, 4-amino-2,2,6,6-tetramethylpiperidine-1-oxyl; tempol, 4-hydroxy-2,2,6,6-tetramethylpiperidine-1-oxyl.

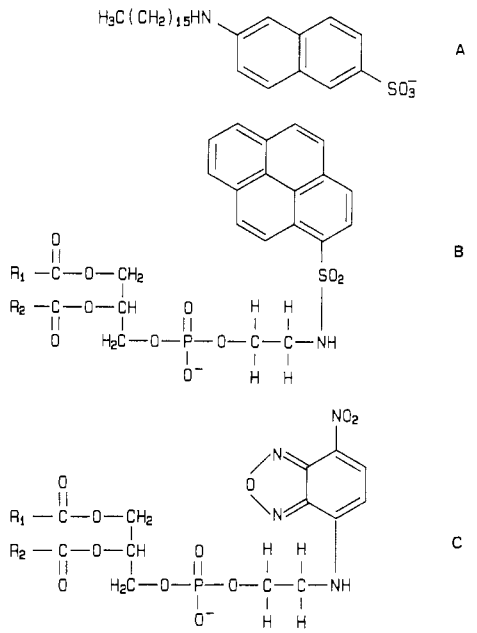

FIGURE 2: Chemical structures of fluorescent lipid analogues with chromophores located near the membrane surface: (A) HNS; (B) pyrenesulfonyl-PE; (C) NBD-PE. R_1 and R_2 represent acyl chains.

(tempamine), and 4-hydroxy-2,2,6,6-tetramethylpiperidine-1-oxyl (tempol) from Molecular Probes (Eugene, OR). Thallium(I) nitrate ($TlNO_3$) was obtained from Alfa Products (Danvers, MA). The structures of HNS, pyrene-PE, and NBD-PE are illustrated in Figure 2. NBD-PE bears a single negative charge at neutral pH (Chattopadhyay & London, 1987). Aqueous solutions, prepared with deionized and filtered 18 MΩ·cm water (Super-Q, Millipore Corp., Bedford, MA), were buffered to pH 7.4 with 0.5–5 mM MOPS.

We used the following molecular weights in our calculations: PS, 832; PG, 775; PC, 787; HNS, 469; pyrene-PE, 1007; G_{M1}, 1545; NBD-PE, 905; gramicidin D, 1974.

G_{M1} was purified as described previously (Myers et al., 1984) from bovine brain gangliosides after exhaustive treatment with *Vibrio cholerae* neuraminidase, which hydrolyzes all polysialogangliosides to monosialogangliosides.

Preparation of Fluorescently Labeled Gangliosides. G_{M1} was dissolved to a concentration of 1 mM and oxidized for 10 min at 0 °C in a solution containing 10 mM $NaIO_4$, 0.1 M sodium acetate (pH 5.5), and 0.15 M NaCl (Veh et al., 1977). The reaction was stopped by adding glycerol to a final concentration of 1.6 M. The solution was passed through a small reverse-phase cartridge (Sep-Pak C_{18}; Waters Associates Inc., Milford, MA) to adsorb the gangliosides. The salts and other water-soluble solutes were removed by eluting with water, and the gangliosides were then eluted with methanol (Williams & McCluer, 1980). The methanol was removed under a stream of nitrogen, and the gangliosides were redissolved to a concentration of 1 mM in the acetate buffer solution described above. Anthraniloylhydrazine was already present in the buffer solution used to redisperse the gangliosides; dansylhydrazine was added from a concentrated stock solution in 2-methoxyethanol. The molar concentration ratio of fluorescent hydrazine reagents to G_{M1} was 10:1. These solutions were incubated overnight at room temperature (~23 °C) after which a 3-fold molar excess of $NaBH_3CN$ (over G_{M1}) was added to drive the coupling reaction. $NaBH_3CN$ reduces Schiff bases but not aldehydes at pH ~6 (Borch et al., 1971). After ~8 h, the solution pH was raised to 8 and a 20-fold molar excess of KBH_4 was added to reduce all unlabeled aldehydes. After incubation at room temperature for

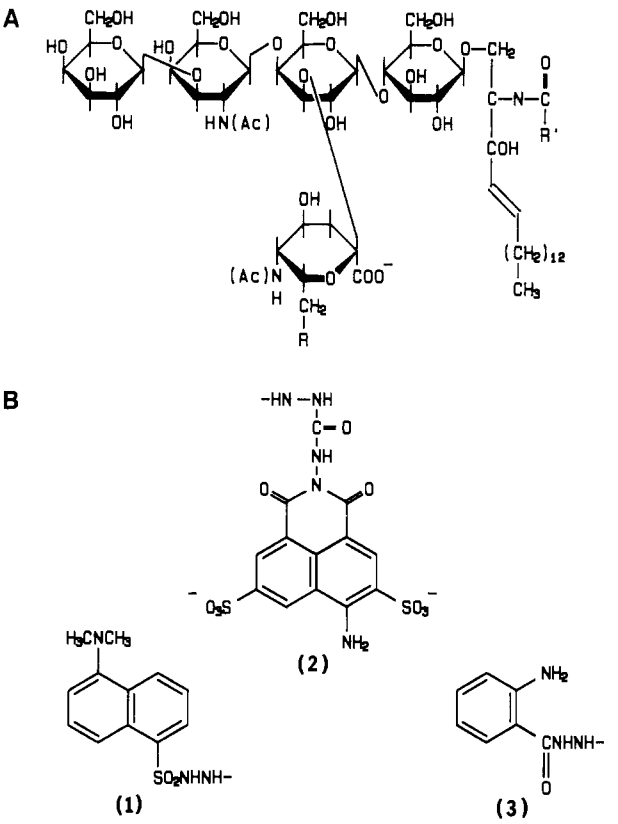

FIGURE 3: (A) Structures of fluorescently labeled G_{M1} molecules. R refers to the chromophore attached to the sialic acid. (B) Structures of the fluorescent chromophores: (1) dansyl; (2) Lucifer yellow; (3) anthraniloyl.

1 h, the gangliosides were desalted on Sep-Pak C_{18} cartridges as described above. Preparative TLC on silica gel 60 plates (EM Science, Gibbstown, NJ) developed in $CHCl_3$/CH_3OH/2.5 N NH_4OH (60:40:9 v/v/v) purified the major fluorescent band from unreacted G_{M1} and free fluorescent reagent. Yields ranged from 20% to 50% for these two fluorescent gangliosides. Lucifer yellow–G_{M1} was synthesized according to the method of Spiegel (1985) with the following modifications: we used Sep-Pak C_{18} cartridges to desalt the gangliosides and reverse-phase C_{18} TLC plates from Whatman (Clifton, NJ) with a developing solvent of CH_3OH/H_2O (4:1) for final purification. In our hands both the published and modified procedures produced very low yields of Lucifer yellow–G_{M1} (~3%). The amounts of fluorescent gangliosides were determined from their molar extinction coefficients (5000, 4500, and 11 900 M^{-1} for anthraniloyl, dansyl, and Lucifer yellow, respectively). All labeled gangliosides used for the experiments ran as a single, fluorescent, resorcinol-positive spot on silica gel TLC. Spiegel et al. (1984b) have confirmed that the fluorescent moieties of hydrazine compounds are linked to only the sialyl residues of G_{M1} by repeating the labeling procedure with asialo-G_{M1} and showing that no fluorescent derivatives were produced. The structures of the fluorescent ganglioside derivatives are illustrated in Figure 3.

Electrophoretic Mobility Measurements. Multilamellar vesicles (MLVs) for microelectrophoresis experiments were prepared according to the method of Bangham et al. (1974). The mobilities of the vesicles were measured in a Rank Brothers Mark I instrument (Bottisham, Cambridge, U.K.) as described previously (McLaughlin et al., 1981). All mobilities reported are the average of at least two sets of measurements on 10 vesicles. We calculated the ζ potential from the electrophoretic mobility, u, using the Helmholtz–Smoluchowski equation (Aveyard & Haydon, 1973; Hunter, 1981)

$$\zeta = \eta u/(\epsilon_0 \epsilon_r) \quad (6)$$

where η is the viscosity of the aqueous solution. For a large, smooth vesicle with charges at the interface, the ζ potential is the average electrostatic potential at the hydrodynamic plane of shear (Overbeek & Wiersema, 1967; O'Brien & White, 1978), which is located 0.2 nm from the surface (Eisenberg et al., 1979; Alvarez et al., 1983; Rooney et al., 1983).

Preparation of Unilamellar Vesicles. Fluorescent probes and gramicidin D were mixed with either egg PC, bovine PS, or egg PG in chloroform or chloroform/methanol mixtures, evaporated to dryness, and placed under vacuum overnight. The lipids were vortexed in a few milliliters of the appropriate salt solution to produce MLVs. They were then either sonicated (Barenholz et al., 1977) to produce highly curved vesicles of ~250-Å diameter or were taken through five cycles of freezing (liquid N_2) and thawing (40 °C water bath) followed by extrusion (10 cycles) through two stacked 0.1-μm polycarbonate filters in an Extruder (Lipex Biomembranes, Inc., Vancouver, BC) to produce large unilamellar vesicles (LUVs) of ~1000-Å diameter (Hope et al., 1985; Mayer et al., 1985).

Fluorescence Measurements. We measured the effect of water-soluble, positively charged quenchers on the fluorescence of probes that were either located at the membrane surface or attached to the sialic acid residue of G_{M1}. We used the Stern–Volmer equation to calculate the aqueous concentration of quencher adjacent to the fluorophore, $[Q]_f$, from the fluorescence measurements

$$(F_0/F) - 1 = K_{SV}[Q]_f \quad (7)$$

where F_0 and F are the fluorescence intensities in the absence and presence of quencher, $[Q]_f$ is the aqueous concentration of quencher adjacent to the fluorophore, and K_{SV} is the Stern–Volmer quenching constant (Lakowicz, 1983).

The fluorescence lifetimes of anthraniloyl-G_{M1} in neutral (PC) and negative (PG) membranes were nearly identical (data not shown). In control experiments with tempamine and anthraninoyl-G_{M1}, we also found that the electrostatic potential deduced from lifetime measurements on PG (−41 mV) was similar to the potential determined from steady-state fluorescence measurements on PS bilayers (−43 mV, see Table II). This is an important control because lifetime measurements are not susceptible to inner filter artifacts.

For a fluorophore completely accessible to a collisional quencher, a plot of $(F_0/F) - 1$ vs $[Q]_\infty$ yields a straight line, where $[Q]_\infty$ refers to the concentration of the quencher in the bulk aqueous phase. The ratio of the slopes of these lines for negative (PS or PG) and neutral (PC) membranes is equal to the Boltzmann factor, $\exp(-\mathcal{F}\Delta\psi_f/RT)$, when the quencher is a monovalent cation. $\Delta\psi_f$ is the difference between the electrostatic potentials the chromophore experiences in a charged and a neutral membrane.

Available spectral evidence indicates that the chromophore of either HNS (our unpublished experiments) or the octadecyl version of this probe (Waggoner & Stryer, 1970) is at the membrane–solution interface. The chromophores of fluorescent phospholipids are near the membrane surface because they are linked chemically to the polar head group [see Figure 2 and Chattopadhyay and London (1987)]. We used thallous and tempamine ions (see Figure 4) to quench the fluorescence from probes (<1 mol %) in membranes.[2] We chose tempamine (see Figure 4), which contains a nitroxide radical, and thallium because they quench fluorescence effectively (Moore & Raftery, 1980; Luisetti et al., 1979), they do not bind significantly to the membrane surface (see Results), and they quench the fluorescence mainly by collisional interactions (Parker, 1968; Berlman, 1973; Green et al., 1973). These quenchers do have some minor drawbacks. Thallium is not sufficiently soluble in chloride solutions for our experiments, and tempamine has the nitroxide radical on the opposite side of the molecule from the protonated primary amine. Furthermore, when the concentration of tempamine is greater than 1 mM, it significantly increases the optical density of the sample, necessitating corrections for an inner filter effect (Appendix). Our experiments on sonicated and extruded vesicles were done in solutions containing either 0.1 M $NaNO_3$/5 mM MOPS (pH 7.4) or 0.01 M $NaNO_3$/0.5 mM MOPS (pH 7.4). Gramicidin D (0.5 mol %) in the vesicles allowed Tl to diffuse across the membranes. Thallium and tempamine were added from stock aqueous solutions of $TlNO_3$ or tempamine acetate (pH 7). Steady-state fluorescence measurements were made with a Spex Fluorocomp (Edison, NJ). Lifetime measurements were obtained with an ORTEC (Oakridge, TN) 9200 system.

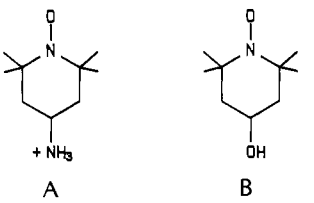

FIGURE 4: Structures of quenchers: (A) tempamine; (B) tempol.

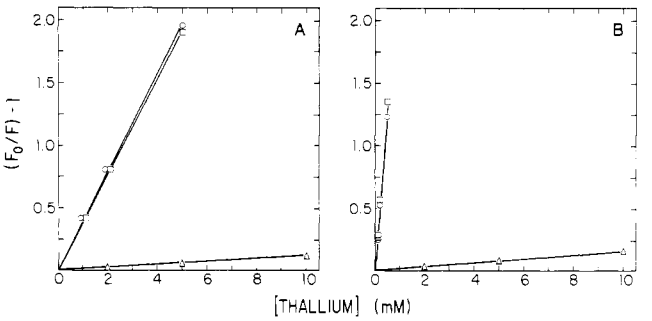

FIGURE 5: Thallium quenching of fluorescence from HNS (1 mol %) in sonicated unilamellar vesicles formed from PC (triangles), PS (squares), or PG (circles). The aqueous solutions contained 0.1 M $NaNO_3$ (A) or 0.01 M $NaNO_3$ (B) buffered to pH 7.4 at 25 °C with 5 or 0.5 mM MOPS, respectively.

RESULTS

Quenching of Fluorophores Located at the Membrane–Solution Interface. Figure 5 illustrates the effect of thallium on the fluorescence of HNS molecules incorporated into the membranes of sonicated unilamellar vesicles (SUVs). Similar results were obtained with tempamine (data not shown). These cations quench the fluorescence more effectively when HNS is in negative (PS or PG) than when it is in neutral (PC) membranes. The negative surface charges attract these positive quenchers; this increases their concentration at the surface and enhances the quenching of fluorophores located at the interface.

The linearity of the Stern–Volmer plots suggests all the fluorophores are accessible to the quenchers. We expected this result: the chromophore should be at the membrane–solution interface rather than buried within the membrane. Furthermore, membranes are permeable to the unprotonated

[2] We considered a number of positively charged quenchers for this study, but most were unsuitable. For example, the monovalent cesium ion quenches too weakly (data not shown), and the divalent transition-metal ions Co^{2+} and Ni^{2+} bind strongly to membrane surfaces and change the surface potential at the concentrations needed for significant quenching (Homan & Eisenberg, 1985).

Table I: Measurements of $\Delta\psi_f$ Obtained from Quenching the Fluorescence of Probes Located at the Surface of PC, PS, and PG Lipid Bilayers[a]

lipid	probe	quencher	[$NaNO_3$] (M)	$\Delta\psi_f$ (mV) SUVs	$\Delta\psi_f$ (mV) LUVs
PS	HNS	thallium	0.1	−87	−86
PG	HNS	thallium	0.1	−89	
PS	HNS	tempamine	0.1	−77	−75
PG	HNS	tempamine	0.1	−75	
PS	pyrene-PE	tempamine	0.1	−77	−75
PG	pyrene-PE	tempamine	0.1	−78	
PG	NBD-PE	tempamine	0.1	−73	
PS	HNS	thallium	0.01	−132	−137
PG	HNS	thallium	0.01	−130	−134
PS	HNS	tempamine	0.01	−128	−128
PG	HNS	tempamine	0.01	−122	−127
PS	pyrene-PE	tempamine	0.01	−130	
PG	pyrene-PE	tempamine	0.01	−129	

[a] Reported values are the average of two measurements, except for NBD-PE and all results for LUVs, which are single measurements.

form of tempamine, and the ionophore gramicidin D allows thallium to diffuse into the vesicles.

The lines in Figure 5 represent least-squares fits to the data points. We used the slopes to calculate the difference between electrostatic surface potentials of the charged and neutral membranes, $\Delta\psi_f$: from eq 5 and 7 the ratio of the slopes is equal to $\exp(-\mathcal{F}\Delta\psi_f/RT)$. We present the calculations for HNS and two fluorescently labeled phospholipids in Table I.[3] The average surface potentials of PS bilayers in 0.1 and 0.01 M $NaNO_3$ are −80 and −131 mV,[4,5] respectively; values that agree well with the results of other techniques (Nir et al., 1978; Ohki & Suave, 1978; Eisenberg et al., 1979; Kurland et al., 1979; McDaniel et al., 1984; Winiski et al., 1986). Furthermore, the change in potential observed when we reduced the salt concentration from 0.1 to 0.01 M agrees with the predictions of the Gouy–Chapman–Stern theory (−76 mV in 0.1 M monovalent salt and −134 mV in 0.01 M monovalent salt, assuming the Na-PS association constant is 1 M^{-1}).

The Gouy–Chapman theory, which includes an assumption that the charges are in a plane, overestimates the magnitude of the potential produced by charges on the surface of a sphere; the overestimate depends on the ratio of vesicle radius to the Debye length (Ohshima et al., 1982). To check for this effect, we repeated some experiments using LUVs of average diameter ~1000 Å. These results, also shown in Table I, agree very well with the results from sonicated vesicles.

Two additional control experiments support the use of quenching measurements to estimate electrostatic potential. First, a neutral analogue of tempamine, tempol (see Figure 4), quenches the fluorescence of HNS and pyrene-PE equally well (within 5%) in neutral and charged membranes (data not shown). Second, the excitation and emission spectra of these probes are almost identical in neutral and charged membranes (data not shown), which indicates the probes are in similar environments.

[3] We obtained similar surface potential results in 0.1 M NaCl and 0.1 M $NaNO_3$ from tempamine quenching of pyrene-PE in PG membranes (−77 and −78 mV).

[4] Thallium quenches pyrene-PE and NBD-PE too weakly in PC membranes for us to reliably measure $\Delta\psi_f$ (Table I).

[5] The surface potentials calculated from measurements with tempamine were not as negative as those calculated from measurements with thallium (Table I). This may be due to the separation between the quenching moiety (nitroxide radical) and the charged group (protonated primary amine): the nitroxide radical may be a significant distance from the surface when the protonated amine is at the membrane–solution interface.

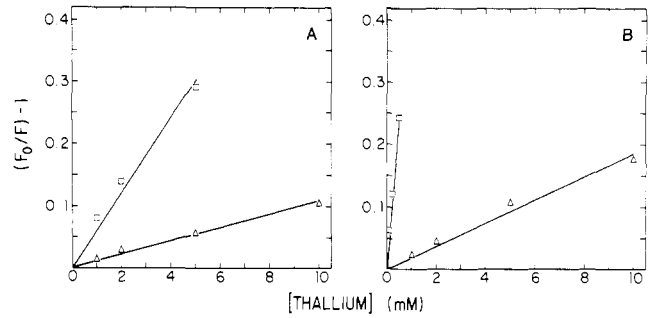

FIGURE 6: Thallium quenching of fluorescence from anthraniloyl-G_{M1} (1 mol %) in extruded unilamellar vesicles formed from PC (triangles) or PS (squares). The lines represent least-squares fits to the data points. The aqueous solutions contained 0.1 M $NaNO_3$ (A) or 0.01 M $NaNO_3$ (B) buffered to pH 7.4 at 25 °C with 5 or 0.5 mM MOPS, respectively.

Table II: Measurements of $\Delta\psi_f$ Obtained from Quenching the Fluorescence of Probes Attached to the Sialic Acid of G_{M1} in PC and PS Lipid Bilayers[a]

probe	quencher	[$NaNO_3$] (M)	$\Delta\psi_f$ (mV)
anthraniloyl	thallium	0.1	−43
dansyl	thallium	0.1	−30
Lucifer yellow	thallium	0.1	−10
anthraniloyl	tempamine	0.1	−43
dansyl	tempamine	0.1	−41
Lucifer yellow	tempamine	0.1	−10
anthraniloyl	thallium	0.01	−86
Lucifer yellow	thallium	0.01	−39
anthraniloyl	tempamine	0.01	−93
Lucifer yellow	tempamine	0.01	−37

[a] Results for anthraniloyl-G_{M1} are the average of two measurements. All other results are single measurements.

Electrophoretic Mobility Measurements. In our analysis of the data we assumed that thallium and tempamine do not affect significantly the electrostatic potential of the membranes. We confirmed this assumption by measuring the effect of these quenchers on the electrophoretic mobilities of PC and PS vesicles. The ζ potentials were calculated from the mobilities by using the Helmholtz–Smoluchowski equation (see Materials and Methods). In 0.1 M $NaNO_3$ at 25 °C, the ζ potentials of PC and PS membranes were −3 and −59 mV, respectively. After addition of thallium to 10 mM, they were −2 and −56 mV, respectively; after addition of tempamine to 10 mM, they were and +1 and −56 mV, respectively. In 0.01 M $NaNO_3$ at 25 °C, the ζ potentials of PC and PS membranes were −2 and −104 mV, respectively. After addition of thallium to 1 mM, they were −2 and −101 mV, respectively; after addition of tempamine to 1 mM, they were +1 and −100 mV, respectively.

Quenching of Fluorophores Attached to Ganglioside. Figure 6 illustrates the effect of thallium on the fluorescence of anthraniloyl-G_{M1} incorporated into the membranes of LUVs formed from either PC or PS. Similar results were obtained with tempamine (data not shown). The degree of quenching is lower for the neutral PC membranes than for the negatively charged PS membranes. However, the ratio of the slopes for PS and PC membranes is smaller than for probes located at the membrane surface (compare Figures 6 and 5), indicating a less negative electrostatic potential in the vicinity of this sialic acid linked anthraniloyl moiety. The results for anthraniloyl-G_{M1}, dansyl-G_{M1}, and Lucifer yellow–G_{M1} are presented in Table II. For example, anthraniloyl-G_{M1} and dansyl-G_{M1} estimate potentials of −43 and −35 mV, respectively, in 0.1 M $NaNO_3$, while anthraniloyl-G_{M1} estimates a potential of −89 mV in 0.01 M $NaNO_3$ (averages of thallium and tempamine results). Lucifer yellow estimates lower potentials;

averaging experimental values for all the probes gives −30 and −64 mV for 0.1 and 0.01 M $NaNO_3$, respectively. The Gouy–Chapman theory predicts that the potentials 1 nm from membranes with surface potentials of −80 and −131 mV (average of results for PS membranes in 0.1 and 0.01 M $NaNO_3$) are −24 mV and −74 mV, respectively; these predictions agree qualitatively with the experimental results obtained from fluorescent gangliosides.

Two control experiments support our approach. First, tempol quenches equally (within 3%) the fluorescence from anthraniloyl-G_{M1} in PC and PS membranes. Second, the excitation and emission spectra of the fluorescent gangliosides are nearly identical in PC and PS membranes, and spectral evidence indicates that these probes are in an aqueous environment. Specifically, the peak of the emission spectrum of anthraniloyl-G_{M1} is red-shifted by 10–12 nm (relative to a methanol solution, where the emission maximum is at 428 nm) when the fluorescent lipid is in vesicles formed in 0.1 M $NaNO_3$. In addition, the widths at half-height of the emission spectra of anthraniloyl-G_{M1} and dansyl-G_{M1} increase 7 nm for this increase in solvent polarity. The labeling reagent anthraniloylhydrazine exhibits identical spectral changes when measured in methanol and $NaNO_3$ solutions. The excitation and emission spectra of Lucifer yellow–G_{M1} in membranes are identical with those of the labeling reagent Lucifer yellow carbohydrazide in aqueous solutions; both emission maxima are red-shifted by 4 nm with respect to this labeling reagent in CH_3OH.

We encountered some experimental difficulties with our sample of dansyl-G_{M1} because the chromophore hydrolyzed when the ganglioside was in PS membranes. The blue shift in the emission spectra and TLC analysis suggest that the breakdown product is dansylsulfonic acid (Avigad, 1977). This hydrolysis is sufficiently slow in 0.1 M $NaNO_3$ (only ~10% breakdown over several hours in the extruded vesicles) that quenching experiments can be performed. In 0.01 M $NaNO_3$, however, this hydrolysis is faster, and we could not do the experiment. Fortunately, anthraniloyl-G_{M1} and Lucifer yellow–G_{M1} are chemically stable in both 0.1 and 0.01 M $NaNO_3$.

Discussion

We used fluorescence quenching measurements to estimate the electrostatic potential adjacent to charged bilayer membranes. When the fluorophores were located at the membrane–solution interface of lipid bilayers, we observed good agreement with previous experimental measurements of surface potential. When the fluorophores were attached to a residue located 1 nm from the interface, we observed qualitative agreement with the predictions of the Gouy–Chapman theory.

We consider our measurements of potential with anthraniloyl-G_{M1} and dansyl-G_{M1} to be the most reliable because their fluorescent moieties are small and neutral. The potentials measured with these probes were more negative than the predictions of the Gouy–Chapman theory. There are at least three possible explanations for this discrepancy. First, we have ignored the finite size of the polar head groups of the phospholipids; counterions in the diffuse double layer may be partially or completely excluded from this head-group region. Second, the neutral chromophores could be located 0.5–0.8 nm instead of 1 nm from the membrane surface because of their width and the length of the chemical linkage between the chromophore and C7 of the sialic acid. Third, the Debye length could be longer than the theoretically predicted values for distances <2 nm from the surface.

On the other hand, Lucifer yellow–G_{M1} measured potentials that were lower than the predictions of the Gouy–Chapman theory. Lucifer yellow is a large molecule with a long carbohydrazide linkage, and it has two negative charges. It may be repelled from the negatively charged surface, and the effect should be more pronounced in solutions of low ionic strength. For example, the results could be explained if Lucifer yellow were located 1.8 and 2.5 nm from the surface in 0.1 and 0.01 M monovalent salt solutions. Other explanations are possible.

In summary, the neutron diffraction experiments of Hentschel et al. (1985), our fluorescence measurements, and the electron spin resonance measurements of Altstiel and Landsberger (1987) do not provide a definitive test of the Gouy–Chapman theory: we can only state that the available data do not contradict the predictions of the theory for distances <2 nm from the surface. We hope to refine the resolution of the fluorescence experiments by making energy-transfer measurements of the distance between the fluorescent groups on NBD-PE and anthraniloyl-G_{M1} (Langner, London, and McLaughlin, unpublished experiments).

Our approach might be useful for measuring electrostatic potentials 1 nm from the surface of reconstituted and biological membranes: gangliosides spontaneously incorporate into the outer monolayer of membranes by transfer from micelles (Felgner et al., 1981; Spiegel et al., 1984a; Spiegel, 1985), and there is no significant fluorescence from cells at the excitation/emission wavelengths of these probes.

Appendix

In our experiments the inner filter effect due to tempamine cannot be ignored. This effect is comparable to the decrease in the intensity of fluorescence due to quenching by tempamine at all concentrations of the quencher. If we assume that the fluorometer records fluorescence only from molecules in the center of the cuvette, we can correct for the inner filter effect using the equation

$$F_{cor} = F_{obsd} 10^{0.5(A_{ex} + A_{em})} \quad \text{(A1)}$$

where F_{cor} is the corrected fluorescence intensity, F_{obsd} is the measured fluorescence intensity, and A_{ex} and A_{em} are the absorbances of the sample at the excitation and emission wavelengths [see, for example, Lakowicz (1983), eq 2.4]. However, it is more correct for us to assume

$$F_{cor} = F_{obsd} 10^{(aA_{ex} + bA_{em} + c)} \quad \text{(A2)}$$

where a, b, and c are constants, characteristic of a given fluorometer, that depend on geometrical factors.

We can then write

$$F_{cor,0} = F_{cor}(1 + k[Q]) \quad \text{(A3)}$$

where $F_{cor,0}$ is the corrected fluorescence in the absence of quencher, k is the Stern–Volmer quenching constant, and [Q] is the concentration of quencher.

We wish to calculate the value of k from the ratio of the observed fluorescence in the absence ($F_{obsd,0}$) and presence of quencher (F_{obsd}). For this purpose we require the values of the constants a and b.

In other words, from eq A2 and A3 we obtain

$$F_{obsd,0}/F_{obsd} = (1 + k[Q]) 10^{(a\Delta A_{ex} + b\Delta A_{em})} \quad \text{(A4)}$$

where ΔA_{ex} and ΔA_{em} are the absorbances due to the quencher, which in our case was tempamine. We determined the values of a and b by measuring the ratio of the fluorescence illustrated on the left-hand side of eq A4 at different wavelengths. The values of the absorbances at these wavelengths were measured independently with a Gilford Instrument 250 spectrophotometer: a and b were calculated by plotting $\log(F_{obsd,0}/F_{obsd})$ against ΔA_{ex} and ΔA_{em}, respectively (see eq A4). We used

tempamine as the quencher and NBD-PE, pyrene-PE, and anthraniloylhydrazine as fluorophores. We obtained similar results in all cases and determined that $a = b = 0.41 \pm 0.03$, a value that agrees within experimental error with the value of $a = 0.45$ measured independently by using a different technique [see Lakowicz (1983), Figure 2.14) on the same fluorometer.

Registry No. **1**, 111689-10-2; **2**, 111689-08-8; **3**, 111689-09-9; G_{M1}, 94458-59-0; ANT hydrazine, 1904-58-1; dansylhydrazine, 33008-06-9.

REFERENCES

Altstiel, L. D., & Landsberger, F. R. (1987) *Biochemistry* (submitted for publication).

Alvarez, O., Brodwick, M., Latorre, R., McLaughlin, A., McLaughlin, S., & Szabo, G. (1983) *Biophys. J. 44*, 333–342.

Aveyard, R., & Haydon, D. A. (1973) *Introduction to the Principles of Surface Chemistry*, pp 40–57, Cambridge Press, Cambridge, U.K.

Avigad, G. (1977) *J. Chromatogr. 139*, 343–347.

Bangham, A. D., Hill, M. W., & Miller, N. G. A. (1974) *Methods Membr. Biol. 1*, 1–68.

Barenholz, Y., Gibbes, D., Litman, B. J., Goll, J., Thompson, T. E., & Carlson, F. D. (1977) *Biochemistry 16*, 2806–2810.

Berlman, I. B. (1973) *J. Phys. Chem. 77*, 562–567.

Borch, R. F., Bernstein, M. D., & Durst, H. D. (1971) *J. Am. Chem. Soc. 93*, 2897–2904.

Cafiso, D. S., & Hubbell, W. L. (1981) *Annu. Rev. Biophys. Bioeng. 10*, 217–244.

Chattopadhyay, A., & London, E. (1987) *Biochemistry 26*, 39–45.

Coronado, R. (1986) *Annu. Rev. Biophys. Biophys. Chem. 15*, 259–277.

Davies, J. T. (1951) *Proc. R. Soc. London, A A208*, 224–247.

Eisenberg, M., Gresalfi, T., Riccio, T., & McLaughlin, S. (1979) *Biochemistry 18*, 5213–5223.

Evans, E. A., & Parsegian, V. A. (1986) *Proc. Natl. Acad. Sci. U.S.A. 83*, 7132–7136.

Felgner, P. L., Freire, E., Barenholz, Y., & Thompson, T. E. (1981) *Biochemistry 20*, 2168–2172.

Fromherz, P. (1973) *Biochim. Biophys. Acta 323*, 326–334.

Fromherz, P. (1987) *Methods of Enzymology; Biomembranes, Biological Transport* (Colowick, S. P., & Kaplan, N. O., Eds.) (in press).

Fromherz, P., & Masters, B. (1974) *Biochim. Biophys. Acta 356*, 270–275.

Green, J. A., Singer, L. A., & Parks, F. H. (1973) *J. Chem. Phys. 58*, 2690–2695.

Hartley, G. S., & Roe, J. W. (1940) *Trans. Faraday Soc. 36*, 101–109.

Hartsel, S. C., & Cafiso, D. S. (1986) *Biochemistry 25*, 8214–8219.

Hentschel, M. P., Mischel, M., Oberthur, R. C., & Buldt, G. (1985) *FEBS Lett. 193*, 236–238.

Homan, R., & Eisenberg, M. (1985) *Biochim. Biophys. Acta 812*, 485–492.

Hope, M. J., Bally, M. B., Webb, G., & Cullis, P. R. (1985) *Biochim. Biophys. Acta 812*, 55–65.

Hunter, R. J. (1981) *Zeta Potential in Colloid Science*, Academic, New York.

Israelachvili, J. N. (1985) *Intermolecular and Surface Forces*, Academic, New York.

Kjellander, R., & Marcelja, S. (1986) *Chem. Phys. Lett. 127*, 402–407.

Klapper, I., Hagstrom, R., Fine, R., Sharp, K., & Honig, B. (1986) *Proteins 1*, 47–59.

Kurland, R., Newton, C., Nir, S., & Papahadjopoulos, D. (1979) *Biochim. Biophys. Acta 551*, 137–147.

Lakowicz, J. R. (1983) *Principles of Fluorescence Spectroscopy*, Plenum, New York.

Loosley-Millman, M. E., Rand, R. P., & Parsegian, V. A. (1982) *Biophys. J. 40*, 221–232.

Luisetti, J., Mohwald, H., & Galla, H.-J. (1979) *Biochim. Biophys. Acta 552*, 519–530.

Maggio, B. (1985) *Biochim. Biophys. Acta 815*, 245–258.

Maggio, B., Cumar, F. A., & Caputto, R. (1981) *Biochim. Biophys. Acta 650*, 69–87.

Marra, J. (1986) *J. Phys. Chem. 90*, 2145–2150.

Marra, J., & Israelachvili, J. N. (1985) *Biochemistry 24*, 4608–4618.

Mayer, L. D., Hope, M. J., Cullis, P. R., & Janoff, A. S. (1985) *Biochim. Biophys. Acta 817*, 193–196.

McDaniel, R. V., & McIntosh, T. J. (1986) *Biophys. J. 49*, 94–96.

McDaniel, R. V., McLaughlin, A., Winiski, A. P., Eisenberg, M., & McLaughlin, S. (1984) *Biochemistry 23*, 4618–4624.

McLaughlin, S. (1977) *Curr. Top. Membr. Transp. 9*, 71–144.

McLaughlin, S., Mulrine, N., Gresalfi, T., Vaio, G., & McLaughlin, A. (1981) *J. Gen. Physiol. 77*, 445–473.

Moore, H.-P. H., & Raftery, M. A. (1980) *Proc. Natl. Acad. Sci. U.S.A. 77*, 4509–4513.

Myers, M., Wortman, C., & Freire, E. (1984) *Biochemistry 23*, 1442–1448.

Nir, S., Newton, C., & Papahadjopoulos, D. (1978) *Bioelectrochem. Bioenerg. 5*, 116–133.

O'Brien, R. W., & White, L. R. (1978) *J. Chem. Soc., Faraday Trans. 2 74*, 1607–1626.

Ohki, S., & Sauve, R. (1978) *Biochim. Biophys. Acta 511*, 377–387.

Ohshima, H., Healy, T. W., & White, L. R. (1982) *J. Colloid Interface Sci. 90*, 17–26.

Overbeek, J. Th. G., & Wiersema, P. H. (1967) in *Electrophoresis, Theory, Methods, and Applications* (Bier, M., Ed.) Vol. II, pp 1–51, Academic, New York.

Parker, C. A. (1968) *Photoluminescence of Solutions*, pp 437–438, Elsevier, Amsterdam.

Pashley, R. M., McGuiggan, P. M., Ninham, B. W., Brady, J., & Evans, D. F. (1986) *J. Phys. Chem. 90*, 1637–1642.

Rooney, E. K., East, J. M., Jones, O. T., McWhirter, J., Simmonds, A. C., & Lee, A. G. (1983) *Biochim. Biophys. Acta 728*, 159–170.

Spiegel, S. (1985) *Biochemistry 24*, 5947–5952.

Spiegel, S., Kassis, S., Wilchek, M., & Fishman, P. H. (1984a) *J. Cell Biol. 99*, 1575–1581.

Spiegel, S., Schlessinger, J., & Fishman, P. H. (1984b) *J. Cell Biol. 99*, 699–704.

Vaz, W. L. C., Nicksch, A., & Jahnig, F. (1978) *Eur. J. Biochem. 83*, 299–305.

Veh, R. W., Corfield, A. P., Sander, M., & Schauer, R. (1977) *Biochim. Biophys. Acta 486*, 145–160.

Verwey, E. J. W., & Overbeek, J. Th. G. (1948) *Theory of the Stability of Lyophobic Colloids*, Elsevier, Amsterdam.

Waggoner, A. S., & Stryer, L. (1970) *Proc. Natl. Acad. Sci. U.S.A. 67*, 579–589.

Williams, M. A., & McCluer, R. H. (1980) *J. Neurochem. 35*, 266–269.

Winiski, A. P., McLaughlin, A. C., McDaniel, R. V., Eisenberg, M., & McLaughlin, S. (1986) *Biochemistry 25*, 8206–8214.

Wynn, C. H., & Robson, B. (1986) *J. Theor. Biol. 123*, 221–230.